

**REPORT DOCUMENTATION PAGE**

*Form Approved  
OMB No. 0704-0188*

The public reporting burden for this collection of information is estimated to average 1 hour per response, including the time for reviewing instructions, searching existing data sources, gathering and maintaining the data needed, and completing and reviewing the collection of information. Send comments regarding this burden estimate or any other aspect of this collection of information, including suggestions for reducing the burden, to Department of Defense, Washington Headquarters Services, Directorate for Information Operations and Reports (0704-0188), 1215 Jefferson Davis Highway, Suite 1204, Arlington, VA 22202-4302. Respondents should be aware that notwithstanding any other provision of law, no person shall be subject to any penalty for failing to comply with a collection of information if it does not display a currently valid OMB control number.

**PLEASE DO NOT RETURN YOUR FORM TO THE ABOVE ADDRESS.**

<b>1. REPORT DATE (DD-MM-YYYY)</b>	<b>2. REPORT TYPE</b>	<b>3. DATES COVERED (From - To)</b>
------------------------------------	-----------------------	-------------------------------------

<b>4. TITLE AND SUBTITLE</b>	<b>5a. CONTRACT NUMBER</b>
	<b>5b. GRANT NUMBER</b>
	<b>5c. PROGRAM ELEMENT NUMBER</b>

<b>6. AUTHOR(S)</b>	<b>5d. PROJECT NUMBER</b>
	<b>5e. TASK NUMBER</b>
	<b>5f. WORK UNIT NUMBER</b>

<b>7. PERFORMING ORGANIZATION NAME(S) AND ADDRESS(ES)</b>	<b>8. PERFORMING ORGANIZATION REPORT NUMBER</b>
---	---

<b>9. SPONSORING/MONITORING AGENCY NAME(S) AND ADDRESS(ES)</b>	<b>10. SPONSOR/MONITOR'S ACRONYM(S)</b>
	<b>11. SPONSOR/MONITOR'S REPORT NUMBER(S)</b>

**12. DISTRIBUTION/AVAILABILITY STATEMENT**

**13. SUPPLEMENTARY NOTES**

**14. ABSTRACT**

**15. SUBJECT TERMS**

<b>16. SECURITY CLASSIFICATION OF:</b>			<b>17. LIMITATION OF ABSTRACT</b>	<b>18. NUMBER OF PAGES</b>	<b>19a. NAME OF RESPONSIBLE PERSON</b>
<b>a. REPORT</b>	<b>b. ABSTRACT</b>	<b>c. THIS PAGE</b>			<b>19b. TELEPHONE NUMBER (Include area code)</b>

## HT-FED2004-56582

### A MINICHANNEL HEAT EXCHANGER SYSTEM FOR HEATING, BOILING, AND SUPERHEATING WATER BY RADIANT COMBUSTION

Mikel L. Sawyer, Ph.D.  
 Applied Research Associates, P.O. Box 40128  
 Tyndall AFB, FL 32403, (850) 283-3725

Aly H. Shaaban, Ph.D.  
 Applied Research Associates, P.O. Box 40128  
 Tyndall AFB, FL 32403, (850) 283-3702

Reza Salavani  
 Air Force Research Lab (AFRL/MLQD)  
 139 Barnes Dr, Suite 2, Tyndall AFB, FL 32403

*Keywords: boiling, two phase, heat transfer coefficient, critical heat flux, minichannel heat exchanger, microchannel, superheating, wetted area, heated area*

#### ABSTRACT

A minichannel steam generator is being developed for a fuel reformer. The reformer will convert jet fuel to a hydrogen-rich stream for a 10 kW fuel cell. A first model has been built and tested. It was a once-through design with of two sequential heat exchangers. Exhaust gases produced saturated liquid in the first unit. The second surrounded a radiant propane burner. The system heated 1.2 to 2.6 gm/s of de-ionized water to more than 650 °C at exit pressures from 106 to 240 kPa. These flows and temperatures meet the requirements for the 10 kW fuel reformer.

The minichannel system operated across three regimes: liquid heating, boiling, and superheating. It used multiple channels in parallel. At certain locations, the number of the parallel channels was changed to restrain the total pressure drop. The channel hydraulic diameter was 0.14 cm. The Reynolds number for the water ranged from 620 to 1,260 in the boiling section and from 1,260 to 3,140 in the superheating section, based on averaged fluid properties. The total pressure drop in the heat exchanger pair ranged from 470 to 870 kPa. The water absorbed heat fluxes ranging from 0.3 to 1.2 W/cm<sup>2</sup> in the single-phase regions and 4.7 to 9.8 W/cm<sup>2</sup> in the boiling region. These values were based on the wetted wall area. The boiling data falls in the range of published results for similar mass flux. An increased capacity for absorbing heat flux was demonstrated as coolant mass flux or Reynolds number increased.

This paper also discusses the reasons for calculating heat flux based on heated area and based on wetted channel area. The need to identify clearly the basis of heat flux is addressed.

#### NOMENCLATURE

$A_c$	[cm <sup>2</sup> ]	Cross sectional area, perpendicular to the flow.
CHF	[W/cm <sup>2</sup> ]	Critical heat flux
Exh-HX		The first of two heat exchangers in the present system. Fluid first enters this unit. Exhaust gasses heat it.
$D_H$	[cm]	Hydrodynamic diameter, ( $4 * \text{flow\_area} / \text{wetted\_perimeter}$ )
G	[gm/(cm <sup>2</sup> · s)]	Mass flux of heated fluid (water)
h	[cm]	Height of rectangular channel
HTC	[W/(cm <sup>2</sup> · C)]	Fluid heat transfer coefficient, based on the wetted wall area, as typical
$k_{\text{fluid}}$	[W/(cm · C)]	Thermoconductivity of fluid
$Nu = HTC * D_H / k_{\text{fluid}}$		Nusselt number
NTU		Number of transfer units, a dimensionless parameter used to evaluate the performance of heat exchangers
ONB		Onset of nucleate boiling
OFI		Onset of flow instability
PT		Pressure transducer
$q''_{\text{wet}}$	[W/cm <sup>2</sup> ]	Heat flux based on the wetted wall area, all four sides of the rectangular channels
$q''_{\text{heated}}$	[W/cm <sup>2</sup> ]	Heat flux based on the flat area between the heat source and the channels
Rad-HX		The second of two heat exchangers. Fluid enters this unit after the Exh-HX. It is heated by radiation and convection.
$Re = G * D_H / \mu$		Reynolds number

$R^2$		R-squared, measurement of the ability of an equation fit by regression to match the source data. $0 \leq R^2 \leq 1$
T	[°C]	Temperature
TC		Thermocouple
w	[cm]	Width of rectangular channel
$w_c$	[cm]	Center-to-center spacing of adjacent channels in a heat exchanger; includes thickness of the separating wall.
$x_{\text{enter}}$		Entrance length
$\mu$	[gm/(cm · s)]	Dynamic viscosity of fluid

## INTRODUCTION

Building heat exchanger channels with smaller hydraulic diameters changes the flow dynamics and brings the bulk fluid in closer contact with the heat exchanger wall. The objective is a higher heat transfer coefficient. Of course, this benefit is paid through a higher pressure drop. The term microchannel has been applied to a wide range of channel sizes. However, Kandlikar suggested a more strict definition that compares a channel's diameter against the mean free path of common gases (Kandlikar, 2003). He defined microchannels to have hydraulic diameters between 10  $\mu\text{m}$  and 200  $\mu\text{m}$ . The term minichannel was used to describe channels with hydraulic diameters between 200  $\mu\text{m}$  and 0.3 cm.

The work presented here has applied minichannel technology to develop a heat exchanger capable of heating, boiling, and superheating water using radiant combustion. Several aspects of mini- and microchannel heat exchangers will be reviewed before the current system is described.

### Configuration and Geometry

Microchannel and minichannel heat exchangers are built in a variety of configurations. Some use a fluid to cool a solid object; others transfer heat between two separate fluids. Others apply electrical or flame heating. One or both fluids may experience a phase change. Some heat exchangers use a single channel while others to divide the flow into multiple channels. Each type has its own applications and challenges.

The influence of channel size on nucleate boiling has been considered in studies at the Argonne National Laboratory (ANL) (Kasza, *et al.*, 1994; Tran, *et al.*, 1994, Tran, *et al.*, 1996). ANL reported that the benefit of smaller channels ( $D_H < 0.3$  cm) is due, in part, to their ability to initiate nucleate boiling sooner and maintain it longer, starting at 3 °C. However, ANL's hypothesis for nucleation in larger channels ( $D_H > 0.3$  cm) was not as cohesive. The experimental work of Kureta, *et al.* (1998) also found nucleate boiling of water to start at slightly lower wall superheat for "small diameter" tubes (0.20 and 0.60 cm).

Bowers and Mudawar (1994a) along with Peng and Peterson (1996) analyzed the geometry and layout of multiple channels for two-phase and single-phase cooling, respectively. The first study used refrigerant R-113, and the second used water.

For multiple, parallel channels Kandlikar (2002) reported temperature and pressure fluctuations as heat flux rose during nucleate boiling. The author attributed these variations to flow reversals caused by uneven vapor generation among the channels. The author reported these reversals based on photographic observations. The reversals occurred in one or more channels compensated by higher forward flow in neighboring channels. Kandlikar believed the flow reversals might be beneficial in some cases. However, the potential for inducing premature critical heat flux should not be overlooked.

Wexler, *et al.*, (2000 and 2003), used an extrusion process to produce a unique polycapillary material (PCM) with numerous small channels. They investigated both boiling and single-phase heating of water flowing at 0.10 to 0.70 gm/s. The surface area density (wetted area/volume) of their four heat exchangers ranged from 7.3 to 62.0  $\text{cm}^2/\text{cm}^3$ . Using a volumetric heat transfer coefficient [ $\text{W}/(\text{cm}^3 \cdot \text{C})$ ], the authors effectively accounted for the higher heat rates experienced as wetted area increased. To report only HTC based on the wetted area [ $\text{W}/(\text{cm}^2 \cdot \text{C})$ ] may not properly compare a tightly packed, high heat rate unit against a heat exchanger with fewer and larger channels. The tightly packed microchannel unit would transfer more heat [W]; however, its HTC might be lower, offset by its greater wetted surface area. Volumetric HTC values up to 6  $\text{W}/(\text{cm}^3 \cdot \text{C})$  were reported for single phase heating of water. Boiling values were 1.4 to 2.6 times higher.

Heat flux must be clearly defined. Often it is not. Two definitions are commonly employed. Several researchers evaluate heat flux based on a smooth area between the heat source and one side of the channels. Other researchers evaluate heat flux using the wetted area that participates in direct heat transfer to the fluid. Each heat flux has its benefits and appropriate applications. The area used for the first heat flux will be called "heated area;" the second will be called "wetted area."

Heat flux based on the heated area is especially useful when attempting to maximize heat transfer through a flat or smooth surface. An example is cooling a microelectronic circuit. Another example is a chemical reaction that is separated from its heat source by a smooth wall (flat or round). In these applications, a prescribed or targeted heat rate is known. The available contact area is then used to specify the required heat flux of the cooling or heating system. Heat flux based on this heated area gives a direct comparison between different microchannel designs. More, densely spaced channels would typically increase the heat transfer [Watts] and increase the heated area heat flux. To the contrary, a heat flux evaluated with the wetted area could decline, giving a wrong impression of the modified heat exchanger.

On the other hand, heat flux based on wetted area is appropriate when evaluating the fundamental performance of the channels. Wetted area heat flux can distinguish the cause of a higher heat transfer rate; whether the cause is a change in phenomena or is only due to greater channel surface area. Authors such as Stoddard, *et al.* (2002) and Yu, *et al.*, (2002)

used wetted-area heat flux when studying the onset of nucleate boiling (ONB), onset of flow instability (OFI), and critical heat flux (CHF) in microchannels. Heat transfer will typically occur on all sides of a rectangular channel and on all portions of a circular channel. For this reason, fluid HTC's are consistently based on the wetted, active area of a channel. Heat flux should be evaluated in the same way when discussing heat transfer phenomena.

### Heat Transfer Regimes in Mini- and Microchannels

Several works have described the flow and heat transfer regimes of forced convection and flow boiling in microchannels (Kandlikar, 2002; Kasza, *et al.*, 1994; Tran, *et al.*, 1994 & 1996; Wadekar, 2001). For a fluid flowing in a heated channel, a single-phase liquid first experiences convective heating. As the liquid reaches its saturation temperature, evaporation slowly starts.

Once the fluid heats and reaches a location where the wall superheat (wall temperature minus fluid saturation temperature) exceeds approximately 3 °C (Tran, *et al.*, 1994) nucleate boiling can begin. Then vapor bubbles form in tiny imperfections on the walls. Small bubbles coalesce into larger bubbles and leave the surface. Further down stream, as evaporation continues, these bubbles join together. Slugs of vapor are formed, separated by liquid. Further boiling results in a core of vapor and mist surrounded by an annulus of liquid wetting the channel walls. This is the annular flow regime. Nucleate boiling can continue in a thin liquid film on the wall (Kandlikar, 2002).

Consider a packet of fluid flowing in a long channel with a constant applied heat flux. As evaporation continues, the remaining liquid has a greater difficulty in wetting the channel wall. The wetting problem results from the disruptive nature of vapor bubbles leaving the hot surface and from Marangoni convection in the remaining liquid film. Because the heat transfer rate of the vapor phase is much lower, the ability of the fluid to cool the wall begins to weaken. Suddenly, the contact between the liquid and the wall ceases. The heat flux drops quickly, and local wall temperature jumps. This rapid event is called a boiling crisis. The maximum local heat flux upstream of the boiling crisis is the critical heat flux (CHF).

Beyond the point of CHF, the walls are dry with only vapor contacting them. If a high vapor quality was reached before CHF, the remaining liquid is entrained as a mist in the bulk vapor flow. The mist evaporates more slowly in this regime. Finally, superheating of the single-phase vapor begins. With wall temperature continuing to rise, the rate of heat transfer begins to rise again. Single-phase convection continues until the fluid exits the heat exchanger.

Two-phase heat transfer offers distinct advantages over single-phase heating. A boiling flow has a higher heat capacity per gram because it absorbs its heat of vaporization. Two-phase cooling offers a higher heat transfer coefficient. Also, fluid evaporation acts to maintain a more uniform wall temperature; whereas, a single phase fluid must rise in

temperature to absorb sensible heat. Qu and Mudawar (2002) and many others have also discussed these benefits.

Kennedy, *et al.* (2000) investigated the initial stages of boiling. They studied the OFI and ONB for sub-cooled water flowing through small tubes of 0.117 cm and 0.145 cm diameter. The data represents the lower values of heat flux required to achieve the early stages of boiling just before exiting the 16 cm length of tubing. In a later work, Stoddard, *et al.* (2002) studied OFI and CHF for water at lower mass flux as it passed through thin horizontal annuli. Hydraulic diameters ranged from 0.145 to 0.200 cm. An electrical heater rod formed the inner surface with heated lengths of 17.4 to 19.7 cm. In this paper, the mass flux rates were similar to those used in current experiments.

In another study of the ONB, Qu and Mudawar (2002) varied flow conditions and visually observed the factors influencing ONB. They developed a model capable of predicting the axial and radial location of the ONB. ONB was defined as the event when vapor bubbles formed only at the exit of the channels. A 1.0 cm wide heat exchanger was used having 21 rectangular channels, 231  $\mu\text{m}$  x 712  $\mu\text{m}$  and 4.48 cm in length. Together these papers indicate the upper range (CHF) and the lower range (ONB or OFI-approximation) of heat flux for boiling in the minichannels used by the authors.

### Critical Heat Flux

One difficulty of a two-phase system is the possibility of reaching critical heat flux. For a cooling system where CHF is to be avoided, the ratio between the expected CHF and the maximum actual heat flux should be greater than 1.3 according to Stultz and Kitto (1992). On the other hand, for a heat exchanger first to boil and then to superheat steam, CHF must be managed rather than avoided. With lower heat flux and higher fluid mass flux, CHF can be delayed until higher vapor quality is achieved.

Several authors have addressed the issue of CHF. Among these works, Wong, *et al.* (1990) described flow and heat flux regimes leading to CHF, and Celata *et al.* (2001) compiled and evaluated over 5000 CHF data. Celata's data included mini-channel results. Bowers and Mudawar (1994a) observed boiling and CHF in parallel channels cooled by R-113. One heat exchanger had channels of 0.254 cm diameter. The other had channels of 510  $\mu\text{m}$  diameter. The same mass flow rate was used with both. The resulting mass flux rates were quite high, 421 and 1840  $\text{gm}/(\text{cm}^2 \cdot \text{s})$ , respectively. CHF was 256  $\text{W}/\text{cm}^2$  for the smaller channels with the higher mass flux, vs. 200  $\text{W}/\text{cm}^2$  for the larger channels. In a complementary work, Bowers & Mudawar (1994b) published a CHF correlation.

Yu, *et al.* (2002) ran a number of CHF experiments in their investigation of water boiling in a single, small horizontal tube of diameter 0.298 cm and 91 cm in length. Mass flux ranged from 5 to 15  $\text{gm}/(\text{cm}^2 \cdot \text{s})$  and CHF from 6.5 to 30.5  $\text{W}/\text{cm}^2$ . CHF increased as mass flux rose.

For a fixed mass flux, applying a uniform but lower heat flux to the channel will delay the CHF until a higher vapor

quality is achieved. This means the CHF will occur further downstream. Consider a series of steady state experiments in a very long heat exchanger. A fixed mass flux of evaporating coolant is used. When a sufficiently low heat flux is applied to the channel, the flowing liquid will boil to a quality of nearly one ( $x \leq 1$ ) without interruption. Then, at CHF the surface temperature would rise, and heat flux would decline after a majority of the liquid evaporated. Only vapor would remain in contact with the channel wall to remove heat. The authors call this event a delayed CHF. In the limit, evaporation would reach completion without CHF. Once vapor alone remains in the channel, heat flux will decline and wall temperature will rise. This event may appear like a CHF, but without any liquid remaining, a term other than CHF should be employed.

In the current experiments, flame combustion provided heat fluxes that were too low for CHF to occur early in the boiling process. Burner performance will be discussed later. A delayed critical heat flux is anticipated in the current experiments given their mass flux rates and the heat source.

## EXPERIMENTAL EQUIPMENT AND PROCEDURES

A steam generator is being developed for a 10 kW fuel reformer for JP-8 jet fuel. The steam generator must supply at least 2.5 gm/s of 650 °C superheated steam at a pressure between 203 and 304 kPa. A first model was built and tested. For ease of fabrication, it was constructed from two separate sections. The first unit was heated by exhaust and is called the "Exh-HX." The second unit surrounded a burner and received radiant heat. It is called the "Rad-HX." Both units are shown in Figure 1. Liquid water was first fed to the bottom of the Exh-HX and then to the Rad-HX, where boiling was completed and superheating was accomplished. The water zigzagged as it passed through horizontal channels and upward through internal, vertical manifolds, exiting at the top of the Rad-HX.

### Heat Exchanger Design

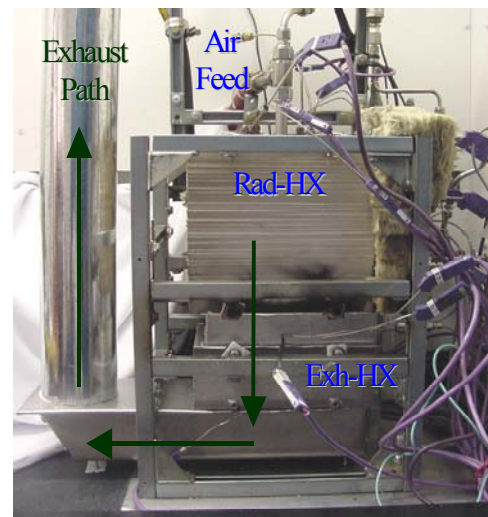
Each of the two heat exchanger units was made from thin plates of 316 stainless steel diffusion bonded together. In half of the plates, narrow channels were cut. The other, solid plates acted as dividing walls. The plates were cut with a water jet. The channel plates and solid plates were alternately stacked. Adjacent channels were connected by holes near the ends of every plate. These holes formed vertical manifolds. To accommodate elevated pressures at high temperatures, external walls were made thick in accordance with the ASME pressure vessel code for rectangular vessels. Fabrication was accomplished at the Air Force Research Laboratory (AFRL).

Changes were made to channel parameters at various locations within the heat exchangers to keep the Reynolds number low as fluid viscosity changed during heating. The goal was to restrain the total pressure drop. The adjustable parameters included (a) width of channel, (b) thickness of plate, which is the height of channel, and (c) the number channels in parallel. Due to the variation in the water jet cut width, the accuracy of the channel width was limited.

Therefore, there was little difference in the hydraulic diameter when parameters were changed. Consequently, only the number of channels in parallel had a net influence on Reynolds number and pressure drop.

The plates in the heating and boiling regions were 0.203 cm thick with channels 0.10 cm wide. In these channels, the hydrodynamic diameter,  $D_H$ , was 0.14 cm. The plates in the superheating region were 0.152 cm thick with channels of 0.15 cm width. The resulting hydrodynamic diameter,  $D_H$ , was 0.15 cm. The average hydrodynamic diameter for the system was 0.14 cm. Minichannels of these sizes are sometimes classified as microchannels in literature. The dividing walls between channels were 0.051 cm thick. In the Exh-HX, four straight channels acted in parallel for liquid heating and early boiling. The channels were 16.8 cm in length. In the Rad-HX, channels were cut with a repeating S-shape with a path length of 26.0 cm. In the boiling section, six channels acted in parallel on each of the two sides of Rad-HX, 12 parallel paths. Finally, in the superheating section, steam flowed through 15 parallel channels on each of the two sides of Rad-HX, 30 parallel paths.

**Figure 1:** Steam Generator Assembly with minimal insulation. Water entered the Exh-HX at the bottom, zigzagged through horizontal channels and vertical manifolds, and finally, exited



at the top, right of the Rad-HX.

The steam generator was a once-through design with no steam drum for recirculation. Water entered the bottom and flowed up and out the top. Within the Exh-HX, the fluid from four parallel channels remixed in each manifold. Before entering the Rad-HX, the fluid divided into two separate, parallel paths, one on each side of the burner. The paths did not re-mix until exiting. Having two paths simplified this heat exchanger. The external plumbing of the Rad-HX is described in Figure 2. Plumbing between the two paths provided a common connection for a single pressure transducer for each elevation. The thinner end walls had no passages.

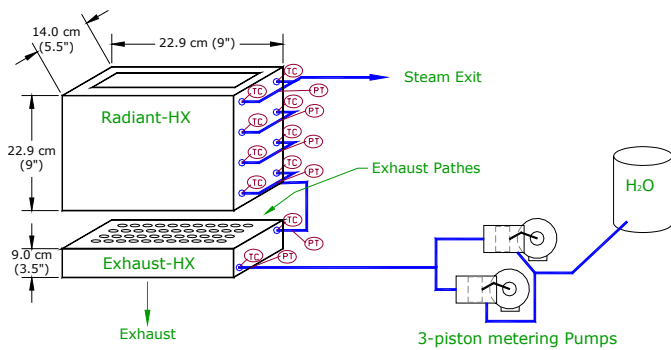


**Figure 2:** Diagram of steam generator system with external plumbing and some instrumentation shown; During operation, the top of Rad-HX was closed, and exhaust flowed downward through the Exh-HX.

### Two-Sided Radiant Burner

A two-sided radiant burner supplied heat. Fuel and air were jointly introduced into the burner to achieve radiant mode heating within its two fiber mesh faces. The burner was fueled by JP-8, a liquid jet fuel, during preliminary experiments. Then, for greater ease, propane was used to generate data for the current report. The system operated with propane flows from 4.8 to 9.0 SLPM and fuel-to-air ratios between 103% and 132% of stoichiometric. At the burner surface, the heat flux was 8 to 14 W/cm<sup>2</sup> during the superheating experiments. These values were based on the lower heating value of propane. The burner heat flux was 6.8 to 13 W/cm<sup>2</sup> when adjusted for the flat, heated area at the base of the channels.

The potential for a premature CHF in the radiant heat exchanger was not a concern with the burner as the heat source. The burner heat flux reduced to the range of 2.6 to 4.6 W/cm<sup>2</sup> when based on the larger, wetted wall area of the channels in the Rad-HX. The actual heat flux values were lower due to heat loss and the transfer of heat to the Exh-HX. At these channel heat flux rates, CHF should occur late in the boiling process given the mass flux rates utilized (Celata, *et al.*, 2001; Wong, *et al.*, 1990; Stoddard, *et al.*, 2002; Qu and Mudawar, 2002). The mass flux rates in the boiling section of Rad-HX were between 5.0 and 10.4 gm/(cm<sup>2</sup> · s). An early CHF, occurring at low steam quality, was unlikely in the current system.

### Pumping and Instrumentation

De-ionized water was pumped using two Eldex model BBB-4 metering pumps, each with a capacity of 1.67 ml/s. During each experiment, the water flow rate was verified by condensing and collecting the exiting steam. The pressure relief valve was observed for leaks to confirm that the full flow reached the heat exchanger system.

At several locations along the flow path, thermocouples (TCs) and pressure transducers (PTs) monitored the state of the water as it was heated. Instrument locations can be seen in Figure 1 and Figure 2. The first two locations were the inlet and outlet of the exhaust heat exchanger, Exh-HX. The radiant

heat exchanger, Rad-HX, had TCs and PTs at its inlet and exit and at two intermediate locations. Each of these four vertical locations had two TCs, one for the front fluid path and one for the rear path. At each vertical TC location, tubing connected the front and rear paths to a single PT.

Temperatures were measured with nickel-chromium versus copper-nickel (type-E) TCs. The TCs and PTs were attached to data acquisition boards mounted in a multiplexing chassis. A computer collected the signals. Data was processed by Labview® software. Data was collected at a rate of 5 scans per second with 15 scans averaged for each recorded data point. Later, two or more of these data points were averaged again to reduce the size of the data file.

After completion of an experiment, data from each instrument was averaged over the 20 to 45 minute time period to give a single data point for each experiment. These averaged results are the data plotted and discussed subsequently.

Heat flux rates were calculated from the heat absorbed by the water using the inlet and exit temperatures. NTU-effective-ness analysis was used to determine exit state of the water leaving the exhaust heat exchanger when partial boiling occurred at this location (Incropera and DeWitt, 1990; Walas, 1990).

### Experimental Procedures

Experiments were initiated by starting the metering pumps, starting data acquisition, and igniting the burner. Once the targeted steam temperature was achieved or exceeded, the system was maintained for 20 to 45 minutes to collect data. The measurements were previously discussed. The exiting steam was condensed with a combination of tap water and ice.

For the superheating experiments, water boiling initiated in the Exh-HX. Then the remainder and majority of the boiling were accomplished in the first portion of the Rad-HX. The upper portion of Rad-HX superheated the steam. TCs at several locations in the flow path allowed the location of boiling to be identified. Figure 2 shows the TC locations. Boiling was complete at the first TC location that indicated mild superheating. The heat flux for this boiling region was evaluated separately from the subsequent region in which only superheating occurred. Due to the fixed number of TCs, the boiling region could not be totally separated from the entire superheating region. Consequently, boiling data for Rad-HX included a few degrees of superheat, but the amount of additional heat absorbed was relatively small.

### RESULTS & DISCUSSION

Water flow rates from 1.2 to 2.6 gm/s were heated from room temperature to more than the 650 °C target, as shown in Table 1. The fluid exited the Rad-HX at 106 to 240 kPa with the exit piping and a cooling coil providing backpressure. The burner and heat exchanger system had a combined thermal efficiency of 70 to 84% based on the lower heating value of propane. In the exhaust heat exchanger, Exh-HX, the exhaust was commonly cooled by 360 °C, e.g.: 480 °C to 120 °C. In these tests, the generator demonstrated its ability to produce

steam at the target flow rate and temperature. The lower flow rates represent a system operating with a partial load. In a second set of experiments, the heat flux and water flow rates were reduced so that the Exh-HX heated water with no boiling. Table 1 also presents these results.

**Table 1:** Steam Generator Performance

Data Set	Water Flow rate	Exh-HX Exit T	Exh-HX Exit steam quality	Rad-HX Avg. Exit T	Thermal Effic. $\frac{Q_{H_2O}}{Q_{fuel}}$	Total Press-ure Drop	Exh-HX Exit Press-ure	Rad-HX Exit Press-ure
	gm/s	C		C	%	kPa	kPa	kPa
SH 1	2.1	144	0.12	678	77%	557	406	150
SH 2	2.6	145	0.08	664	84%	561	417	156
SH 3	1.9	146	0.16	712	75%	541	430	240
SH 4	2.5	152	0.20	703	77%	870	495	168
SH 5	1.2	147	0.13	684	70%	410	438	106
SH 6	1.9	169	0.16	700	70%	840	779	136
Liq 1	1.0	99	< 0.0	-----	-----	10	144	-----
Liq 2	2.0	90	< 0.0	-----	-----	33	160	-----
Liq 3	2.2	105	< 0.0	-----	-----	32	178	-----

NOTES: Water entered 22 to 26 °C at the inlet to Exh-HX.

Exh-HX inlet: “Rad-HX Exit Pressure”+ “Total Pressure Drop.”

“SH” is a superheating experiment.

“Liq” is an experiment with only liquid heating in the Exh-HX.

#### Radiant Heat Exchanger Data

Upon entering the second heat exchanger, Rad-HX, the flow divided into two separate paths. This design resulted in a mal-distribution of flow as observed with thermocouples on either side of RAD-HX. The heat flux rates reported were averaged for both sides because it was not possible to determine the extent of the flow difference between the two sides.

The heat transfer performance of the boiling section of Rad-HX is presented in Figure 3. Each data point is the averaged result from one experiment. Literature data for onset of ONB and OFI give an indication of the lower heat flux limit for boiling. Other data on the graph describe the upper limit of boiling heat flux achieved in earlier studies. These higher values include CHF data. Only the lower portions of Stoddard’s (2002) data sets are shown, but the trend lines were based on the full data sets. The literature data is dependent on the parameters and equipment used by the researchers. The heated length was especially significant in the experiments where heat flux was adjusted to achieve boiling or CHF just at the exit of the channel(s). Even so, the data provides a general comparison of boiling heat flux in minichannels over the range of mass flux rates currently used.

Because the authors described boiling phenomena (ONB, OFI, and CHF), the heat flux rates in Figure 3 were plotted using wetted area. The data of Stoddard, *et al.* (2002) and Yu, *et al.* (2002) were published with this basis. Qu and Mudawar

(2002) chose to use the flat area parallel to the base of the channels to calculate heat flux. Their data were converted before being plotted here.

In Figure 3, the data for boiling and mild superheating from the radiant heat exchanger fall within the upper and lower limits described by Yu, *et al.*, (2002) and Qu and Mudawar (2002). The data fall below the averaged range of Stoddard, *et al.*, (2002). The current heat flux data were an average of the full boiling regime (quality of  $x \geq 0$  to  $x=1$ ) and some superheating. Therefore, the averaged heat flux should be less than the CHF value and greater than incipient boiling heat flux, as observed on the graph.

In Figure 3, the rise of ONB heat flux with increasing mass flux resulted from an increasing capacity of convective heat transfer, delaying boiling. At the upper end of each envelope, boiling maintained higher heat flux before yielding to CHF as mass flux increased. The ability of higher coolant mass flux to absorb higher heat flux is seen in all data sets.

Figure 4 presents the superheating data for the Rad-HX. Heat flux rises with Reynolds number. For comparison, the data for boiling with mild superheating is also included in the graph. This data was discussed previously. The boiling data has higher heat flux at lower Reynolds numbers, demonstrating the advantage of two-phase heat transfer.

Two evaluations of heat flux are shown in Figure 4. One heat flux uses the wetted wall area inside the channels, and the other uses the flat area between the heat source and one side of the channels. The flat area received direct radiant heating from the burner. The difference between these two heat flux rates is the fixed ratio of the areas. This ratio will be different for each heat exchanger design. For the Rad-HX, the ratio is 2.7 m<sup>2</sup>/m<sup>2</sup>.

The boiling section transferred heat to the water at 12 to 20 W/cm<sup>2</sup>, based on the flat, heated area. The superheating section transferred heat to the water at 1.3 to 3.4 W/cm<sup>2</sup>. In comparison, the boiling section transferred 4.7 to 9.8 W/cm<sup>2</sup> based on wetted channel area. The corresponding values in the superheating section ranged from 0.4 to 1.2 W/cm<sup>2</sup>.

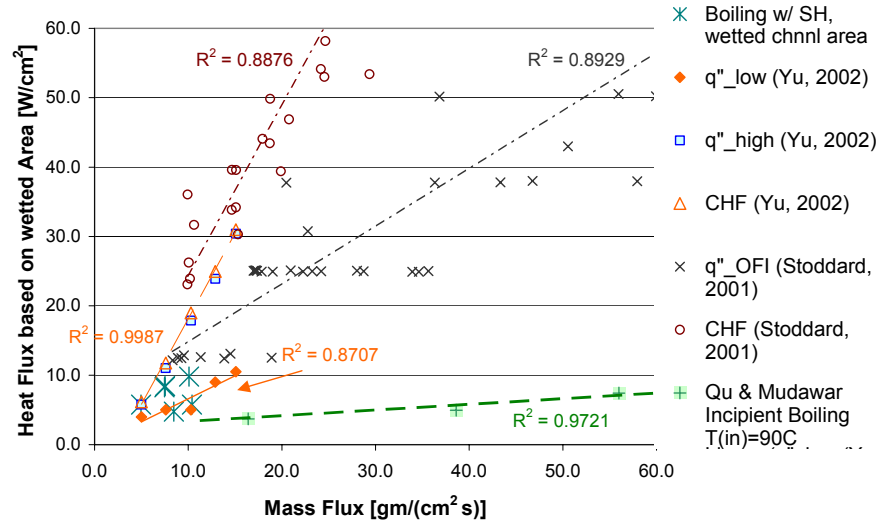
The reader will notice that the boiling heat flux rates plotted in Figure 4 exceeded the maximum heat flux available from the burner. The burner produced up to 13 W/cm<sup>2</sup> when based on the flat, heated area at the base of the channels in the Rad-HX. As shown in the plot, the water absorbed higher flux in the boiling section and a much lower heat flux in the superheating section. This difference occurred because heat was redistributed vertically within the body of the Rad-HX.

The total heat absorbed in the Rad-HX, was, of course, less than the total heat produced by the burner. The remainder of the heat was either absorbed later in the exhaust heat exchanger or lost through insulation and exiting exhaust. The energy balance for the system was maintained.

Thermocouples within the upper section of Rad-HX allowed the overall heat transfer coefficient to be evaluated based on the temperature difference between the fluid and the flat wall facing the heater. The overall HTC data for superheating steam in the Rad-HX are shown in Figure 5. As

expected, results rise with Reynolds number. The values are small due to the large temperature difference required to push heat through the 1.75 cm thick wall separating the fluid and the atmospheric combustion chamber. Catalytic combustion within adjacent channels would bring the heat closer to the steam by

lower thermal resistance and greater heat transfer. Catalytic heating is being pursued for a future design.



requiring only a thin wall for separation. The result would be

**Figure 3:** Boiling and mild superheating data from Rad-HX compared with representative data indicating lower and upper bounds for boiling in minichannels with hydraulic diameters on the order of 0.1 cm (Qu and Mudawar, 2002, Stoddard, *et al.*, 2002, and Yu, *et al.*, 2002). Heat flux rates were based on the wetted wall area. Trend lines were added.

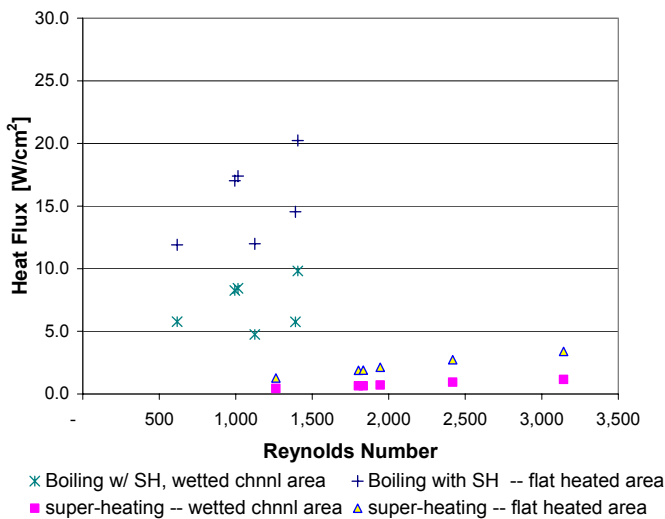


**Figure 4:** Rad-HX data for superheating and for boiling with mild superheating; Heat flux absorbed by the water evaluated using (a) wetted channel area and using (b) the heated area at the base of the channels. Reynolds numbers were based on the average fluid properties in each section of the heat exchanger.

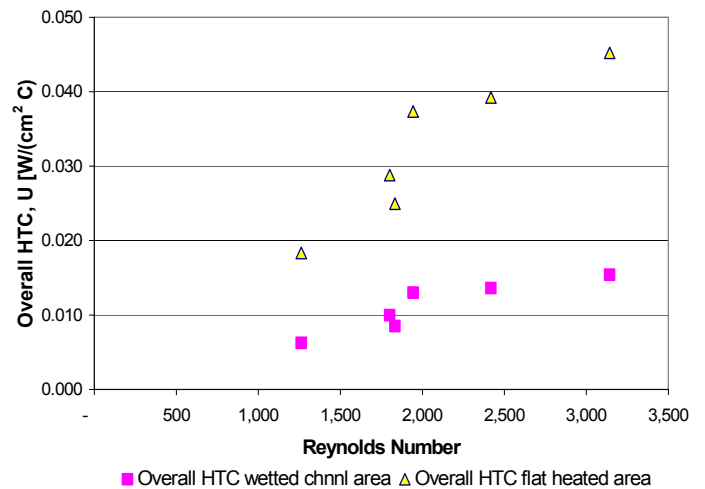


**Figure 5:** Overall heat transfer coefficients for superheating steam in the Rad-HX, based on the temperature difference between the fluid and the flat wall facing the heater.

## Exhaust Heat Exchanger Data

Two groups of heat flux data from the exhaust heat exchanger, Exh-HX, are shown in Figure 6. The first set of data is the heating and initial boiling accomplished during the superheating experiments. These experimental data were taken concurrently with the data in Figure 3, Figure 4, and Figure 5. The heat flux for liquid heating in the Exh-HX was about 30% lower than the heat flux from the single-phase superheating in the Rad-HX. A mild rise of heat flux with mass flux is seen in this data from the Exh-HX. The quality of the partially evaporated water leaving Exh-HX was between  $x = 0.1$  and  $x = 0.2$ . The quality was evaluated using effectiveness-NTU analysis. The second set of data in Figure 6 came from experiments in which water exited Exh-HX with no boiling. The heat generated at the burner was reduced for these experiments.

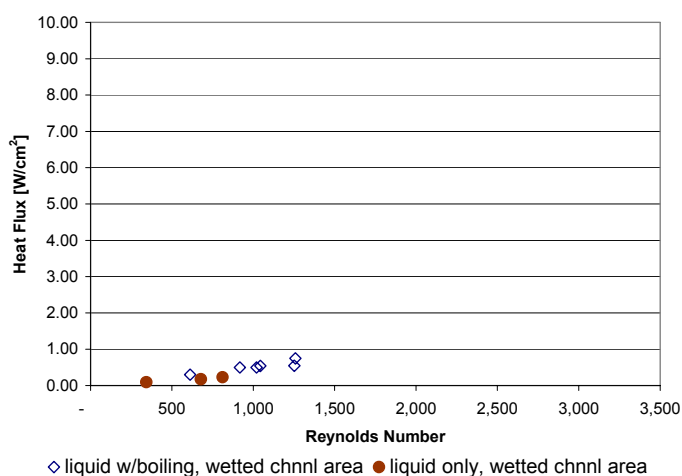


**Figure 6:** Exhaust heat exchanger (Exh-HX) data for (1) experiments with liquid heating & initial boiling combined and (2) experiments with liquid heating only. Heat flux rates were based on the wetted wall area.

Since the Exh-HX is a fluid-to-fluid heat exchanger, heat flux based on heated area has not been calculated. This heat flux is more commonly evaluated for systems that are heated through a simple, often flat, surface as existed in the Rad-HX.

Overall HTC data for Exh-HX are displayed in Figure 7. The HTC was evaluated using the log mean temperature difference between the inlet and exit temperatures of the water and of the exhaust. Data for the superheating section of Rad-HX are shown again for comparison. The flow in the Exh-HX was laminar with Reynolds numbers from 610 to 1260, based on the average fluid properties. For a laminar, single-phase flow that is hydrodynamically fully developed, the heat transfer coefficient is constant ( $Nu = HTC * D_H / k_{fluid} = \text{constant}$ ). For a developing laminar flow, the HTC rises with Reynolds number. In a laminar flow, the hydrodynamic entrance length is estimated by  $x_{enter} = 0.05 * Re * D_H$  (Incropera and DeWitt, 1990). For the lowest flow rate, the Exh-HX entrance length was  $x_{enter} = 0.05 * 400 * 0.14 \text{ cm} = 2.8 \text{ cm}$ . For the highest flow rate, the entry length was 8.8 cm. Each channel in the

Exh-HX was 16.8 cm long, followed by a manifold. The lowest flow rates became fully developed early in the channel. The higher flow rates passed through half the channel before becoming fully developed. Therefore, for the higher flow rates, entrance region effect would have influenced the average HTC. The graph of HTC versus Re is nearly level, but suggests a slight rise with increasing Reynolds number. This mild trend appears to demonstrate entrance region effects, but more data would be necessary to be certain.

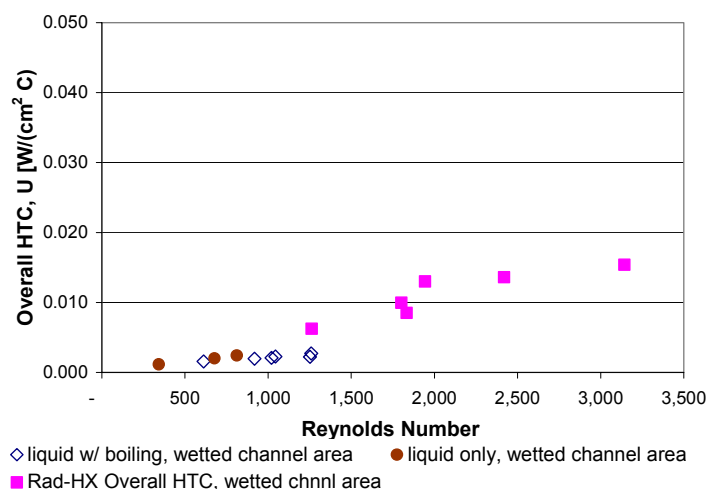


**Figure 7:** Overall HTC for liquid heating and partial boiling in the Exh-HX with superheating data from radiant heat exchanger for comparison.

## CONCLUSIONS

The steam generator model has achieved the flow capacity and outlet temperature required for the 10kW steam reformer. De-ionized water from 1.2 to 2.6 gm/s was superheated to more than 650 °C at pressures of 106 to 240 kPa. The steam generator operated over a range of flow rates representing half loading to full loading of a 10 kW fuel reformer system.

The steam generator demonstrated a practical application of minichannel technology for a challenging heat transfer requirement. The system heated, boiled, and highly superheated water using a once-through design. The generator was made of two units operating in multiple flow and heat transfer regimes. As such, its results are not easily compared against the individual test sections often reported in literature. Improvements will be considered to reduce the system size and weight.

In the radiant heat exchanger, heat was redistributed vertically from the superheating region to the boiling region. So, the boiling region absorbed a greater heat flux than the burner produced. Of course, the total heat balance was maintained. Boiling heat flux data fell within the upper and lower limits reported by two out of three literature sources.

## REFERENCES

- Bowers, M. B. and Mudawar, I., "Two-Phase Electronic Cooling Using Mini-Channel and Micro-Channel Heat Sinks -- Part 1. Design Criteria and Heat Diffusion Constraints," *Trans. ASME, J. Electronic Packaging*, Vol. 116, pp. 290-297, AD 1994a.
- Bowers, M. B. and Mudawar, I., "High Flux Boiling in Low Flow Rate, Low Pressure Drop Mini-Channel and Micro-Channel Heat Sinks," *Int. J. Heat & Mass Transfer*, Vol. 37, No. 2, pp. 321-332, AD 1994b.
- Celata, G. P., Mishima, K., and Zummo, G., "Critical Heat Flux Prediction for Saturated Flow Boiling of Water in Vertical Tubes," *Int. J. Heat and Mass Trans.*, 44, pp. 4323-4331, AD 2001.
- Fedorov, A. G. and Viskanta, R., "Three-Dimensional Conjugate Heat Transfer in the Microchannel Heat Sink for Electronic Packaging," *Int. J Heat Mass Transfer*, 43, pp. 399-415, AD 2000.
- Kandlikar, S. G., "Fundamental Issues Related to Flow Boiling in Minichannels and Microchannels," *Experimental Thermal and Fluid Science*, pp. 389-407, AD 2002.
- Kandlikar, S. G., "Microchannels and Minichannels – History, Terminology, Classification, and Current Research Needs," ICMM2003-1000, First Int. Conf. On Microchannels and Minichannels, Rochester, NY, April 24-25, AD 2003.
- Kasza, K. E. and Wambsganss, W. M., "Development of a Small-Channel Nucleate-Boiling Heat Transfer Correlation," ANL-94/32, Argonne National Laboratory, AD 1994.
- Kennedy, J. E., Roach Jr., G. M., Dowling, M. F., Abdel-Khalik, S. I., Ghiaasiaan, S. M., Jeter, S. M., and Quershi, Z. H., "The Onset of Flow Instability in Uniformly Heated Horizontal Microchannels," *Transactions of the ASME*, Vol. 122, pp. 118-125, AD 2000.
- Kureta, M., Kobayashi, T., Mishima, K., and Nishihara, H., "Pressure Drop and Heat Transfer for Flow-Boiling of Water in Small-Diameter Tubes" *Transactions JSME, Series B*, Vol.63, No.6, pp. 871-879, AD 1998.
- Incropera Frank P. and David P. DeWitt, *Fundamentals of Heat and Mass Transfer*, 3<sup>rd</sup> Ed., John Wiley & Sons, New York, AD 1990.
- Peng, X. F. and Peterson, G. P., "Convective Heat Transfer and Flow Friction for Water Flow in Microchannel Structures", *Int. J. Heat Mass Transfer*, Vol. 39, No. 12, pp.2599-2608, AD 1996.
- Qu, W. and Mudawar, I., "Prediction and Measurement of Incipient Boiling Heat Flux in Micro-Channel Heat Sinks," *Int. J Heat & Mass Trans.*, 45, pp. 3933-3945, AD 2002
- Stultz, S. C. and Kitto, J. B. (eds.), *Steam, Its Generation and Use*, 40th ed., 1st Print, Babcock & Wilcox, AD 1992.
- Stoddard, R. M., Blasick, A. M., Ghiaasiaan, Abdel-Khalik, S. I., S. M., Jeter, S. M. and Dowling, M. F., "Onset of Flow Instability and Critical Heat Flux in Thin Horizontal Annuli," *Experimental Thermal and Fluid Science*, 26, pp.1-14. AD 2002.
- Tran, T.N., Wambsganss, M. W., and France, D. M., "Boiling Heat Transfer in Compact Heat Exchangers," Conf-941128—5, AIChE Annual Meeting AD 1994.
- Tran, T.N., Wambsganss, M. W., and France, D. M., "Small Circular- and Rectangular-channel Boiling with Two Refrigerants," *Int. Journal Multiphase Flow*, Vol. 22, No. 3, pp. 485-498, AD 1996.
- Wadekar, Vishwas V., "Compact Exchangers for Phase Change," HTFS, AEA Technology Hyprotech, Oxfordshire, England, (internet document), AD 2001 (year estimated)
- Walas, Stanley M., *Chemical Process Equipment Selection and Design*, Butterworth-Heinemann, Boston, AD 1990.
- Wexler, E. M., Tuchinsky, L. J., and Loutfy, R. O., "Experimental Study of Heat Transfer Properties of Polycapillary Materials," *Proceedings of IMECE: International Mechanical Engineering Congress & Exposition*, November 5-10, AD 2000.
- Wexler, E., Loutfy, R. O., Ortega, A., Wallinger, D., Prindiville, T., "Novel Boiling-Enhanced Multi-Channel Heat Sinks," TED-AJ03-380, The 6th Annual ASME-JSME Thermal Engineering Joint Conference, JSME, March 16-20, AD AD 2003.
- Wong, Y. L., Groeneveld, C. C., and Cheng, S. C., "CHF Prediction For Horizontal Tubes," *Int. J. Multiphase Flow*, Vol. 16, No. 1, pp. 123-138, AD 1990.
- Yu, W., France, D. M., Wambsganss, M. W., and Hull, J.R., "Two-phase pressure drop, boiling heat transfer, and critical heat flux to water in a small diameter horizontal tube," *Int. J. Multiphase Flow*, Vol. 28, pp. 927-941, AD 2002.